EML Based on Lumped Configuration, Identical Epitaxial Layer and HSQ Planarization

Ali Al-Moathin, Lianping Hou, Eugenio Di Gaetano, and John H. Marsh
James Watt School of Engineering
University of Glasgow
Glasgow G12 8QQ, U.K.
Ali.Al-Moathin@glasgow.ac.uk

***Abstract*—We present a new electroabsorption modulated laser based on a lumped configuration, identical epitaxial layer scheme, and a new low-permittivity planarization method. The design of the device is intended to offer a high modulation frequency using a simple and cheap fabrication process. A thick-film of HSQ spin-on coating was used to planarize the device and enable a low capacitance contact to the p-side. A 6-µm-thick planarized HSQ layer was fabricated and used to implement the electrode to the electroabsorption modulator.**

***Index Terms*—Electroabsorption modulator, electroabsorption modulated laser, identical epitaxial layer, side-wall grating, low-permittivity material, thick-film HSQ planarization**

I. Introduction

An electroabsorption modulated laser (EML) comprises a distributed feedback (DFB) laser and electroabsorption modulator (EAM), integrated monolithically into the same chip. Such sources are attractive because of their compact size, low drive voltage, stable operation and capability to provide high-frequency modulation [1], [2]. EMLs are becoming widely used in long-haul optical communication systems, but the technologies of wavelength division multiplexing (WDM) and high data rates per channel are now required in local area networks (LANs) such as passive optical networks (PONs) supporting 40 Gb/s [3]. There is therefore substantial interest in developing low-cost EMLs and WDM laser arrays to support higher data capacity in LANs [4], [5]. The operation of the EAM is based on the quantum confined stark effect (QCSE) and, in the so-called identical epitaxial layer (IEL) scheme, a common multi-quantum well (MQW) structure is used by both the laser and the EAM [1], [6]. This provides a fast, simple, cost-effective and regrowth-free route to fabrication [1], [7].

The material used in this work is a p-i-n structure grown using the AlGaInAs/InP material system, which was designed for C-band operation (wavelength range 1530-1565 nm). The high characteristic temperature of AlGaInAs MQW lasers provides a solution for uncooled EML operation [1], [6]. This is due to the larger conduction band offset in this material system ($\Delta Ec = 0.72\Delta Eg$) compared to that of the more conventional InGaAsP/InP system ($\Delta Ec = 0.4\Delta Eg$) [6], [8], [9].

This work is supported by the Engineering and Physical Sciences Research Council, UK (grant EP/L015323/1).

Integrating an EAM monolithically using the IEL scheme restricts design flexibility in terms of material compositions and thicknesses. The EAM is conventionally implemented using a lumped element – the so-called lumped electroabsorption modulator (LEAM). Although the design provides simple and low-cost fabrication, it results in a high electrode capacitance, which in turn limits the maximum modulation frequency. The capacitance is directly proportional to the area of the lumped element, which is usually configured with either a circular or rectangular pad. The minimum pad area is constrained by the diameter of the bond wire; generally, a pad size of double that of the bond wire diameter is required.

The capacitance can be reduced by using a low-permittivity-material as the insulator for the bond pad which can also provide the necessary planarization. Conventional planarization methods such as those based on BCB (benzocyclobutene) or polyimide materials are difficult to apply or are incompatible with some photonic integration steps [10]. Another option, Hydrogen Silsesquioxane (HSQ) planarization is commonly used in standard integrated circuits for multilevel metal interconnects [11]. Its chemical similarity to SiO2 has led to it being identified as a material for low-k applications [12]. Based on the spin-on coating technique, film thicknesses up to 800 nm in a single spin can be achieved. Thicker dielectric-films of up to 10 µm can be planarized using the method explained in [10], [13].

Here, an EML device is designed and fabricated based on the IEL scheme and thick HSQ planarization using low-cost and simple fabrication steps. The design allows the bond-pad capacitance to be minimized to achieve the highest possible modulation frequency.

II. Design and Device Structure

A schematic of the device is shown in Fig. 1, where both the DFB and EAM have a single common ridge waveguide of 2.0 μm width and are separated electrically by a 40-μm-long isolation section. The Bragg grating for the DFB laser is implemented with a side-wall grating (SWG), as this approach is simple and flexible and the lasers are capable of delivering powers $>$ 10 dBm [6], [14], [15]. The coupling coefficient κ of the grating is evaluated based on a set of simulations and analytic calculations. Figure 2 shows the simulated κ value as a function of the recess depth. Based

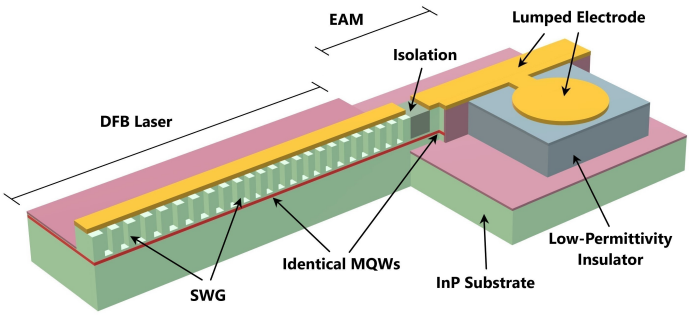

Fig. 1. Schematic of the EML device.

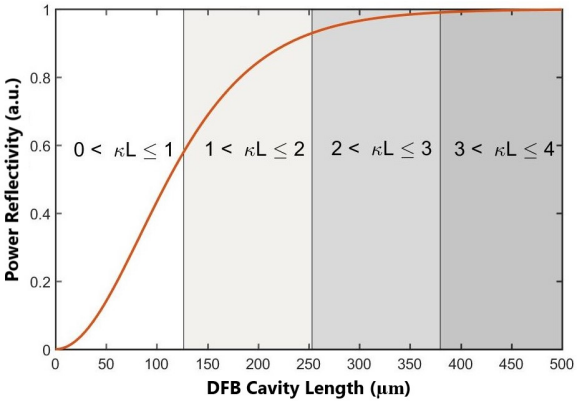

Fig. 3. Optical power reflectivity as a function of DFB cavity length for a ridge waveguide designed with a 0.4 μm recess depth.

on this curve, the grating was designed with a 0.4 μm depth, which provides κ equal to 79 cm^{-1}. The required length of the DFB cavity was determined by considering the κL factor using the power reflectivity relation $R = tanh^2(\kappa L)$ [16]. The curve, plotted in Fig. 3, indicates a length of 400 μm corresponds to $\kappa L = 3.2$ and this was adopted for the design. However, it is found experimentally that the reactive ion etching (RIE) lag effect in dry-etching can reduce κ substantially [17], therefore lasers with 500-μm- and 600-μm-long cavities were also fabricated. A first-order Bragg grating was used, with a quarter-wavelength-shift placed at the centre of the DFB cavity to ensure single-mode lasing (Fig. 6(a)). In order to ensure reliable laser operation, the DFB ridge was shallow-etched. This avoids non-radiative recombination at the sidewalls and minimizes overlap between the optical mode and the side-wall edges, which would result in high scattering losses.

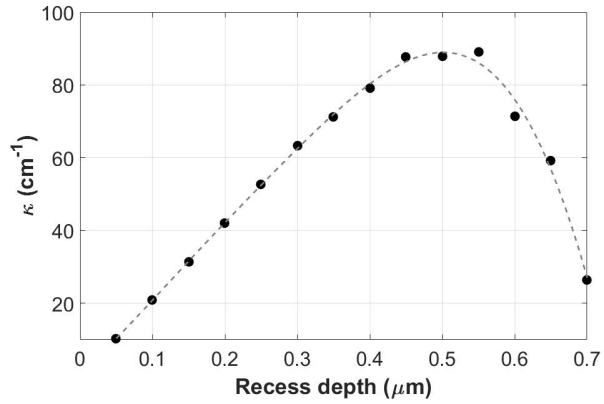

Fig. 2. Coupling coefficient κ as a function of the recess depth for a waveguide with 1.91 μm shallow-etch depth and 2 μm width.

In order to minimize the capacitance, the waveguide in the EAM section is deep-etched. This constrains the junction area of the EAM to be the same as that of the waveguide. The active region of the material, shown in Fig. 4, consists of five AlGaInAs quantum-wells (QWs) that are separated by six AlGaInAs quantum-barriers (QBs). This waveguide core is further sandwiched by upper and lower layers of graded index (GRIN) to form a separate confinement heterostructure

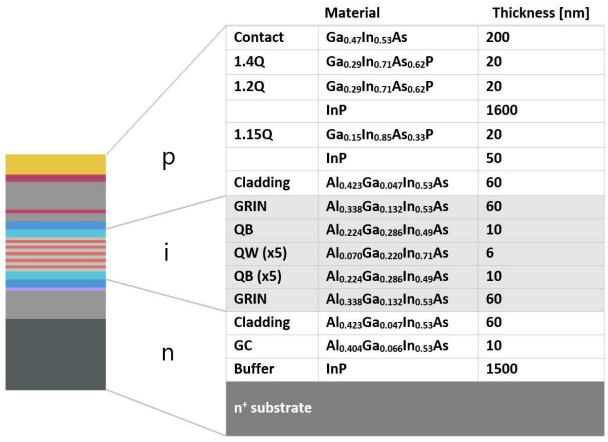

	Material	Thickness [nm]
Contact	$Ga_{0.47}In_{0.53}As$	200
1.4Q	$Ga_{0.29}In_{0.71}As_{0.62}P$	20
1.2Q	$Ga_{0.29}In_{0.71}As_{0.62}P$	20
	InP	1600
1.15Q	$Ga_{0.15}In_{0.85}As_{0.33}P$	20
	InP	50
Cladding	$Al_{0.423}Ga_{0.047}In_{0.53}As$	60
GRIN	$Al_{0.338}Ga_{0.132}In_{0.53}As$	60
QB	$Al_{0.224}Ga_{0.286}In_{0.49}As$	10
QW (x5)	$Al_{0.070}Ga_{0.220}In_{0.71}As$	6
QB (x5)	$Al_{0.224}Ga_{0.286}In_{0.49}As$	10
GRIN	$Al_{0.338}Ga_{0.132}In_{0.53}As$	60
Cladding	$Al_{0.423}Ga_{0.047}In_{0.53}As$	60
GC	$Al_{0.404}Ga_{0.066}In_{0.53}As$	10
Buffer	InP	1500
n+ substrate		

Fig. 4. AlGaInAs/InP epi-layer structure.

with a total active region thickness of 0.21 μm. Accordingly, 2-μm-wide EAMs will have an intrinsic-capacitance of 1.12 pf-μm^{-1}. EAM lengths of 130 μm, 150 μm, and 170 μm were fabricated.

The electrode of the EAM is designed with a circular pad of 60 μm diameter integrated on a thick low-permittivity insulator. The HSQ planarization method explained in [10], is used to fabricate the insulating layer. This approach is for the first time applied here to reduce the bond-pad capacitance in this type of photonic integration. The overall capacitance of the EAM was calculated as a function of the HSQ thickness and the –3 dB cut-off frequency was estimated for a 50 Ω impedance driver. Figures 5(a) and 5(b) show calculations for the EAM capacitance and modulation frequency respectively. The results indicate that increasing the thickness of the HSQ film from 1 μm to 6 μm can increase the modulation frequency by a factor of 1.6.

III. Fabrication

The common ridge waveguide of the EML was first dry-etched to define a 1.91-μm-high ridge waveguide. The Al-containing cladding layer above the active region (Fig. 4) was

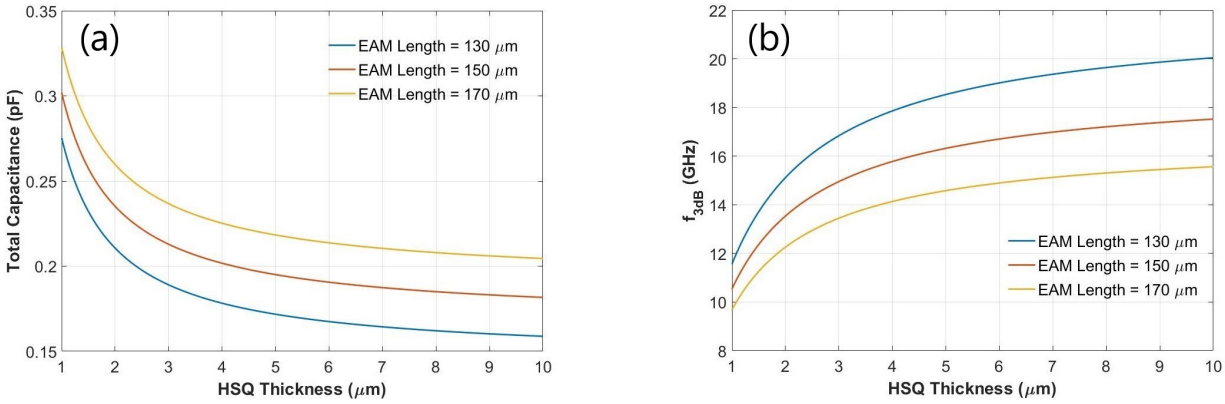

Fig. 5. (a) Total capacitance produced by the EAM as a function of the planarized HSQ thickness, and (b) the estimated modulation frequency calculated as a function of the planarized HSQ thickness.

used as a dry-etch stop-layer by adding O_2 to the dry-etch gas mixture. In the EAM section, an additional etching stage was used to realize a deep-etched ridge. Figure 6(a) shows the shallow-etched DFB SWG, and Fig. 6(b) shows the deep-etched EAM ridge waveguide.

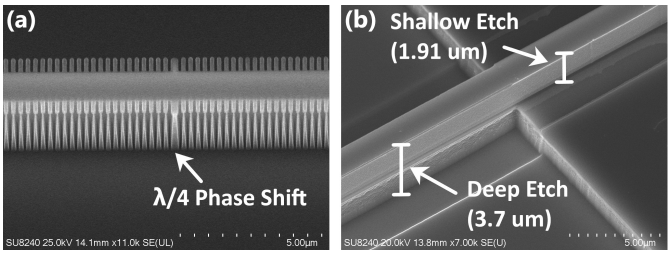

Fig. 6. SEM images for the (a) DFB grating achieved with shallow etch, and (b) the integrated EAM ridge with deep etch.

The isolation section between the DFB laser and the EAM was realized by dry-etching the sample to a depth of 0.24 μm to remove the uppermost GaInAs, 1.4Q, and 1.2Q layers. An HSQ planarized film of 6 μm thickness was achieved with five stages of spin-on coatings. After spinning each layer of HSQ, 40 nm of SiO_2 was deposited using plasma-enhanced chemical vapor deposition (PECVD). Figure 7 shows the sample surface after finishing the HSQ planarization; the figure identifies the DFB laser, isolation section, EAM, and the planarized area. Furthermore, a cross-section of the planarized HSQ is shown in Fig. 8, which indicates the film thickness, distribution, and the position of the HSQ film with respect to the EAM ridge wall.

The p-contacts to the DFB and the EAM were implemented by depositing 30 nm of Ti followed by 33 nm of Pt and 240 nm of Au. The substrate was then thinned manually to leave a device thickness of 120 μm. The n-contact was created by depositing successive layers of Au/Ge/Au/Ni/Au with thicknesses of 14/14/14/11/240 nm respectively. Finally, the sample was annealed at 380 °C for 60 seconds using rapid thermal annealing (RTA). The final device is shown in Fig. 9.

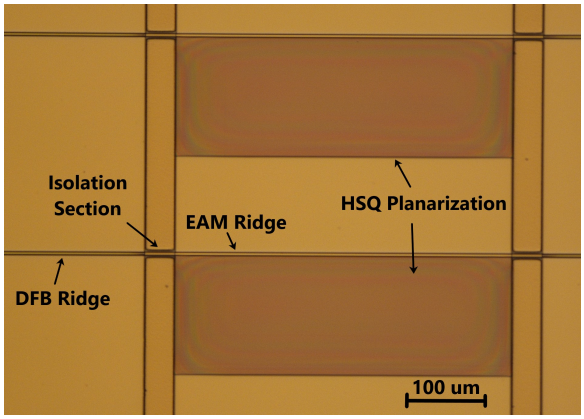

Fig. 7. Sample surface after HSQ planarization.

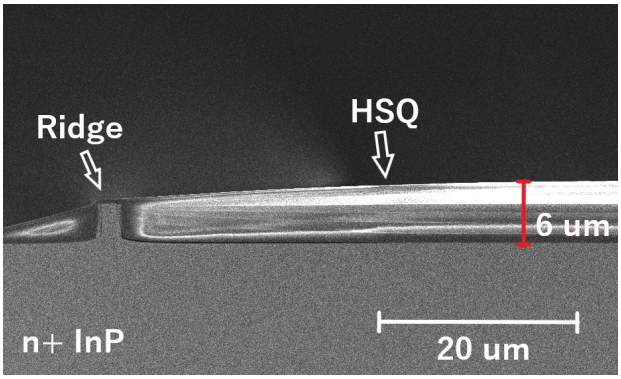

Fig. 8. Cross-section SEM image for the planarized HSQ film.

IV. Conclusion

In conclusion, an EML device has been designed and fabricated based on a combination of the IEL scheme, SWG ridge waveguide, lumped electrode, and a novel planarization technique. By using regrowth-free fabrication processes to reduce the cost of manufacturing, the device should be commercially viable in mass deployment applications such as PONs. A WDM array of the devices can be integrated

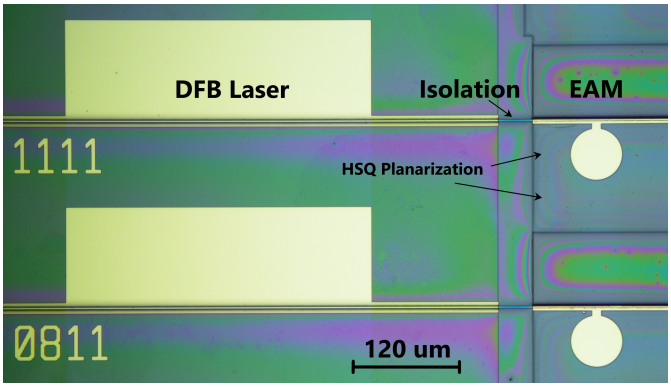

Fig. 9. Final result of the device fabrication.

monolithically with precise wavelength spacing to increase the data capacity. A new planarization method, based on HSQ spin-on coating, has been used for the first time to integrate the bond-pad. The method was implemented using a simple process with no need for high-temperature annealing or etch-back processing and can be used for film thicknesses up to 10 μm. Simulations show this is a promising route for reducing the bond-pad capacitance and can increase EML modulation speeds to $\sim$ 20 GHz using a lumped electrode.

ACKNOWLEDGMENT

The authors would like to acknowledge the staff of the James Watt Nanofabrication Centre at the University of Glasgow for their help and support.

REFERENCES

[1] C. Sun et al., "Fabrication and packaging of 40-Gb/s AlGaInAs multiple-quantum-well electroabsorption modulated lasers based on identical epitaxial layer scheme," J. Light. Technol., vol. 26, no. 11, pp. 1464–1471, 2008.

[2] J. S. Choe, Y. H. Kwon, J. S. Sim, S. B. Kim, and M. H. Lee, "40 Gbps electroabsorption modulated DFB laser with tilted facet formed by dry etching," Conf. Proc. - Int. Conf. Indium Phosphide Relat. Mater., pp. 267–270, 2007.

[3] "40-Gigabit-capable passive optical networks (NG-PON2): General requirements," Reccomendation ITU-T G.989.1 (03/2013), International Telecommunication Union, Geneva (2013).

[4] S. Tang, L. Hou, X. Chen, and J. H. Marsh, "Multiple-wavelength distributed-feedback laser arrays with high coupling coefficients and precise channel spacing," Opt. Lett., vol. 42, no. 9, pp. 1800–1803, 2017.

[5] O. K. Kwon, Y. A. Leem, Y. T. Han, C. W. Lee, K. S. Kim, and S. H. Oh, "A 10 × 10 Gb/s DFB laser diode array fabricated using a SAG technique," Opt. Express, vol. 22, no. 8, pp. 9073–9080, 2014.

[6] L. Hou, M. Tan, M. Haji, I. Eddie, and J. H. Marsh, "EML based on side-wall grating and identical epitaxial layer scheme," IEEE Photonics Technol. Lett., vol. 25, no. 12, pp. 1169–1172, 2013.

[7] A. Ramdane, F. Devaux, N. Souli, D. Delprat, and A. Ougazzaden, "Monolithic integration of multiple-quantum-well lasers and modulators for high-speed transmission," IEEE J. Sel. Top. Quantum Electron., vol. 2, no. 2, pp. 326–335, 1996.

[8] T. Y. and F. K. W. Kobayashi, M. Arai, N. Fujiwara, T. Fujisawa, T. Tadokoro, K. Tsuzuki, "Wide temperature range operation of 10-/40-Gbps 1.55-μm electroabsorption modulator integrated DFB laser," OECC2010 15th, vol. 1, no. July, pp. 9–10, 2010.

[9] W. Kobayashi et al., "Design and fabrication of 10-/40-Gb/s, uncooled electroabsorption modulator integrated DFB laser with butt-joint structure," J. Light. Technol., vol. 28, no. 1, pp. 164–171, 2010.

[10] A. Al-Moathin et al., "Thick film hydrogen silsesquioxane planarization for passive component technology associated with electronic-photonic integrated circuits," J. Vac. Sci. Technol. B, Nanotechnol. Microelectron., vol. 37, no. 6, p. 61210, 2019.

[11] M. J. Loboda, C. M. Grove, and R. F. Schneider, "Properties of a-SiOx:H Thin Films Deposited from Hydrogen silsesquioxane resins," J. Electrochem. Soc., vol. 145, no. 8, pp. 2861–2866, 1998.

[12] C. W. Holzwarth, T. Barwicz, and H. I. Smith, "Optimization of hydrogen silsesquioxane for photonic applications," J. Vac. Sci. Technol. B Microelectron. Nanom. Struct. Process. Meas. Phenom., vol. 25, no. 6, pp. 2658–2661, 2007.

[13] A. Al-Moathin, L. Hou, and J. H. Marsh, "Novel Electroabsorption Modulator Design Based on Coplanar Waveguide Configuration," in 2019 12th UK-Europe-China Workshop on Millimeter Waves and Terahertz Technologies (UCMMT), 2019, pp. 1–3.

[14] J. Wiedmann et al., "1.5 μm wavelength distributed reflector lasers with vertical grating," Electron. Lett., vol. 37, no. 13, pp. 831–832, 2001.

[15] H. Abe, S. G. Ayling, J. H. Marsh, R. M. De La Rue, and J. S. Roberts, "Single-Mode Operation of a Surface Grating Distributed Feedback GaAs—AlGaAs Laser with Variable-Width Waveguide," IEEE Photonics Technol. Lett., vol. 7, no. 5, pp. 452–454, 1995.

[16] M. Zanola, "Tunable and narrow linewidth mm-wave generation through monolithically integrated phase-locked DFB lasers," 2011.

[17] H. Jansen et al., "BSM 7: RIE lag in high aspect ratio trench etching of silicon," Microelectron. Eng., vol. 35, no. 1–4, pp. 45–50, 1997.